Supplemental Figures

Fig. S1

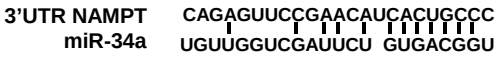

Fig. S2

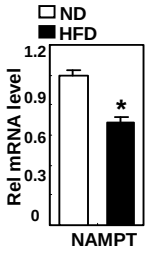

Fig. S3

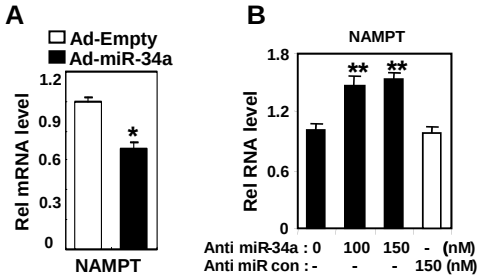

Fig. S4

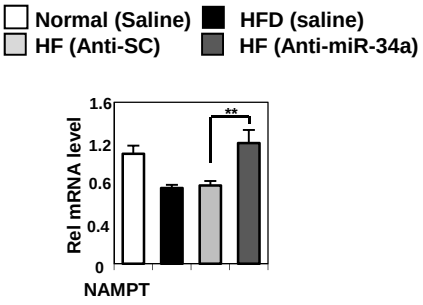

Fig. S5

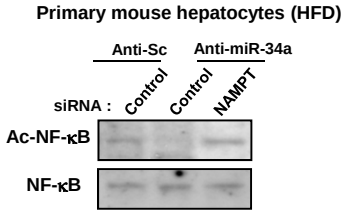

Fig. S6

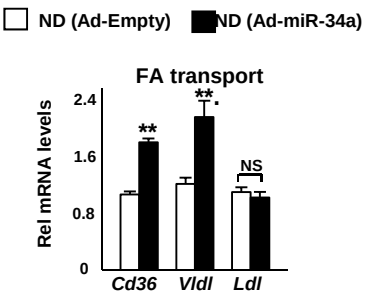

Fig. S7

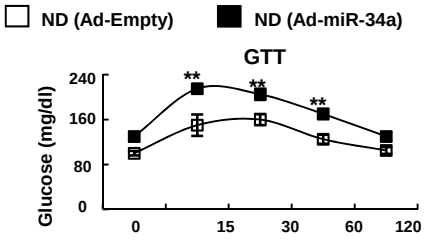

Fig. S8

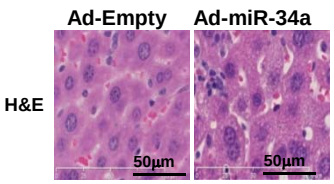

Fig. S9

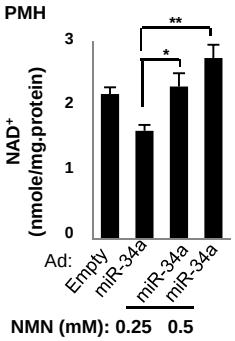

Fig. S10

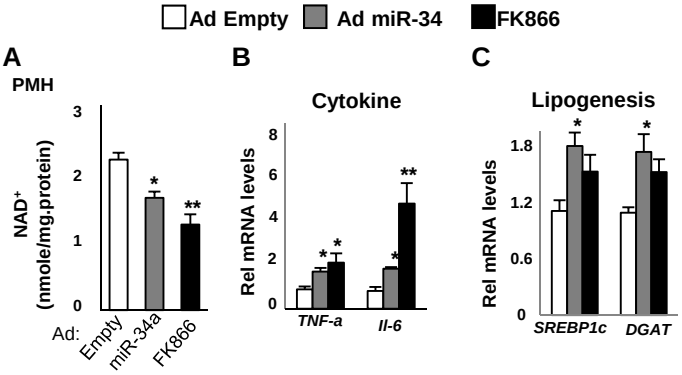

Fig. S11

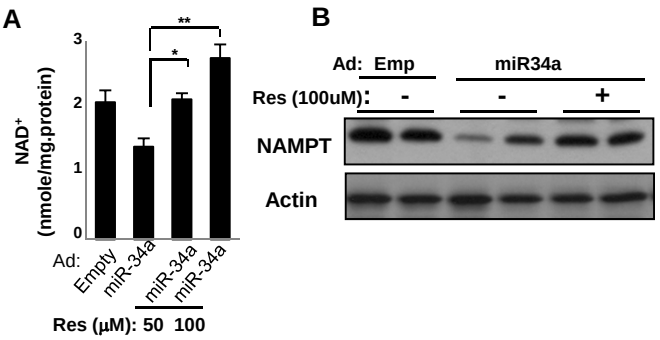

Fig. S12

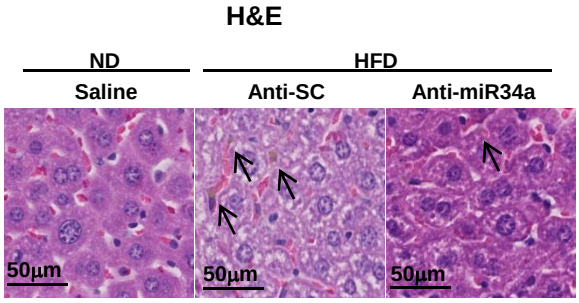

Fig. S13

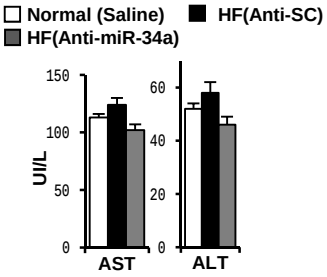

Fig. S14

List of primer sequences of mouse metabolic genes for q-RTPCR

No.	Gene	Forward (5'-3')	Reverse (5'-3')
1	Nampt	CATAGGGGCATCTGCTCATT	GCTGCTGGAACAGAATAGCC
2	Sirt1	AGTTCCAGCCGTCTCTGTGT	GATCCTTTGGATTCCTGCAA
3	Ppar β/δ	AATGCGCTGGAGCTCGATGAC	ACTGGCTGTCAGGGTGGTTG
4	Ppar α	CGAGGTGAAAGATTCGGAAA	GGCCTTGACCTTGTTCATGT
5	Cpt-1	TCGAAACATCTACCATGCAGCA	CAGCATTCTTCGTGACGTTGG
6	Cytc	GGAGGCAAGCATAAGACTGG	TCCATCAGGGTATCCTCTCC
7	Mcad	GATCGCAATGGGTGCTTTTGATAGAA	AGTTGATTGGCAATGTCTCCAGCAAA
8	Srebp1c	GCTGTTGGCATCCTGCTATC	ATGCTGGAAGTGACGGTGGT
9	Dgat	TGGTGTGTGGTGATGCTGATC	GCCAGGCGCTTCTCAA
10	CD36	GCCAAGCTATTGCGACATGA	AAGGCATTGGCTGGAAGAAC
11	Vldl	GAGACCCTGACTGCAAGGAC	GCCGTGGATACAGCTACCAT
12	Bip	TCATCGGACGCACTTGGAA	CAACCACCTTGAATGGCAAGA
13	Chop	GTCCCTAGCTTGGCTGACAGA	TGGAGAGCGAGGGCTTTG
14	Calreticulin	TTACGCACTGTCCGCCAAA	GCTCATGCTTCACCGTGAACT
15	IL-6	AGAAGGAGTGGCTAAGGACCAA	AACGCACTAGGTTTGCCGAGTA
16	Tnf-α	AGCCCCCAGTCTGTATCCTT	GGTCACTGTCCCAGCATCTT
17	Mcp-1	CAGCCAGATGCAGTTAACGC	GCCTACTCATTGGGATCATCTTG
16	36B4	CGACTCACAGAGCAGGC	CACCGAGGCAACAGTTGG

Fig. S15

List of primer sequences of mouse genes for semi-quantitative ChIP assay

No.	Gene	Forward (5'-3')	Reverse (5'-3')
1	Sirt1	GTGTTGTGGTCCGGCCCGC	CTCCGCTCGACGCGCGGCACT
2	Nampt	GAGGATCGGAATCCACAAGA	GGACTGAGGAGGACGTGAG
3	Gapdh	AGTGCCAGCCTCGTCCCGTAGACA	AAGTGGGCCCCGGCCTTCTCCAT

Supplemental Figure Legends

Fig. S1. The 3'UTR of Nampt mRNA contains a miR-34a binding site. Alignments of the miR-34a sequence with the putative miR-34a binding site in the 3'UTRs of mouse Nampt mRNAs are shown.

Fig. S2. Effects of high fat diet on hepatic NAMPT expression. Mice were fed normal chow (ND) or a high fat diet (HFD) for 16 weeks and hepatic NAMPT mRNA levels were measured by q-RTPCR analysis. Statistical significance was determined by the Student's t test (SEM, n=3, *p<0.05).

Fig. S3. Effects of miR-34a on NAMPT expression. (A) Primary hepatocytes were prepared from lean mice and infected with Ad-miR-34a or Ad-empty and 2 days later, mRNA levels of NAMPT were detected by q-RTPCR. (B) Mouse primary hepatocytes were treated with anti-miR-34a or scrambled RNA and 2 days later, NAMPT mRNA levels were detected. Statistical significance was determined by the Student's t test (SEM, n=3, *p<0.05, **, p<0.01).

Fig. S4. Effects of in vivo silencing of miR-34a on NAMPT mRNA levels. Mice were fed normal chow (ND) or a high fat diet (HFD) for 16 weeks and injected via the tail vein with saline, control RNA, or anti-miR-34a oligonucleotides three times at 4-day intervals, and hepatic mRNA levels of NAMPT were detected by q-RTPCR. Statistical significance was determined by the Student's t test (SEM, n=5, *p<0.05, **, p<0.01).

Fig. S5. Effects of downregulation of SIRT1 by siRNA on acetylation of NF-kB. Primary hepatocytes were prepared from diet-induced obese mice and treated with anti-miR-34a or scrambled RNA and then, further treated with control scrambled RNA or SIRT1 siRNA and acetylation levels of NF-kB were detected by IB using acetylated NF-κB (3045) from Cell Signaling Technology. Total NF-kB levels were detected by IB using NF-κB (sc-109R) from Santa Cruz Biotechnology.

Fig. S6. Effects of Ad-miR-34a on expression of FA transport genes. Lean mice were infected with Ad-miR-34a or Ad-empty and 1 week later, mRNA levels of FA transport genes were detected by q-RTPCR. Statistical significance was determined by the Student's t test (SEM, n=5, **, p<0.01).

Fig. S7. Effects of Ad-miR-34a on glucose tolerance. Lean mice were infected with Ad-miR-34a or Ad-empty and 1 week later, glucose tolerance test (GTT) was performed. Statistical significance was determined by the Student's t test (SEM, n=5, **, p<0.01).

Fig. S8. Effects of Ad-miR-34a on liver staining by H&E. Lean mice were infected with Ad-miR-34a or Ad-empty and 1 week later, H&E staining of liver tissue was performed.

Fig. S9. Effects of treatment with NMN on NAD^+ levels. Primary hepatocytes were prepared and infected with Ad-empty or Ad-miR-34a and then, treated with NMN as indicated. Cellular NAD+ levels were measured. Statistical significance was determined by the Student's t test (SEM, n=3, *p<0.05; **, p<0.01).

Fig. 10. Effects of treatment with FK866 on cellular NAD^+ levels. Primary hepatocytes were prepared and infected with Ad-empty or Ad-miR-34a and then, treated with FK866, an inhibitor of NAMPT, as indicated. Cellular NAD+ levels were detected.

Fig. S11. Effects of treatment with resveratrol on NAMPT protein and NAD^+ levels. Primary hepatocytes were prepared and infected with Ad-empty or Ad-miR-34a and then, treated with resveratrol as indicated. Cellular NAMPT protein and NAD+ levels were detected. Statistical significance was determined by the Student's t test (SEM, n=3, *p<0.05; **, p<0.01).

Fig. S12. Effects of anti-miR-34a treatment on liver fat accumulation and macrophage infiltration. Mice were fed normal chow (ND) or a high fat diet (HFD) for 16 weeks and injected with saline, control RNA, or anti-miR-34a three times at 4-day intervals, and treated with control RNA or anti-miR-34a and H&E staining was performed to detect liver histology. Infiltrated macrophages are indicated by arrows.

Fig. S13. Effects of anti-miR-34a treatment on serum AST/ALT levels. Mice were fed normal chow (ND) or a high fat diet (HFD) for 16 weeks and injected via the tail vein with saline, control RNA, or anti-miR-34a three times at 4-day intervals, and treated with control RNA or anti-miR-34a and serum AST and ALT levels were measured by ELISA.

Fig. S14. Primer sequences for q-RTPCR analysis are shown.

Fig. S15. Primer sequences for semi-quantitative PCR for the ChIP assays are shown.